THE JOURNAL OF PHYSICAL CHEMISTRY B

Article

pubs.acs.org/JPCB

Effect of Water Structure on Gelation of Agar in Glycerol Solutions and Phase Diagram of Agar Organogels

Shilpi Boral and H. B. Bohidar*

Polymer and Biophysics Laboratory, School of Physical Sciences, Jawaharlal Nehru University, New Delhi 110 067, India

Supporting Information

ABSTRACT: A comprehensive study of hydration of polyanionic agar molecules in its solution and gel phase in glycerol−water binary solvent is reported. Raman spectroscopy results predict differential water structure arrangement for glycerol−water binary solvent, 0.02% (w/v) agar in glycerol solution and 0.3% (w/v) agar organogel. The 3200 cm^{-1} Raman band pertaining to ice-like structure of water was found to increase in gel phase alike in glycerol−water solvent while it decreased in agar solutions with increase in glycerol concentration. In contrast, the partially structured water corresponding to the component 3310 cm^{-1} of Raman spectra increased in agar solution, and decreased in gel phase similar to glycerol−water solvent case. We have explained these observations based on a simple model where the available oxygen to hydrogen atom ratio in a given solvent−polymer system uniquely defines hydration in solution and gel phases. The gelation concentration was found to increase from 0.18 (for water) to 0.22% (w/v) (50% v/v glycerol solution) as the glycerol concentration was raised. Correspondingly, the gelation temperature, T_g, showed a decline from 40 to 20 °C, and the gel melting temperature, T_m, revealed a reduction from 81 to 65 °C in the same glycerol concentration regime. Two distinctive features are evident here: (i) presence of glycerol as a cosolvent does not favor the gelation of agar as compared to water and (ii) agar organogels are softer than their hydrogels. A unique 3D phase diagram for the agar organogel is proposed. Circular dichroism data confirmed that the agar molecules retained their biological activity in these solvents. Thus, it is shown that thermo-mechanical properties of these organogels could be systematically tuned and adapted as per application requirement.

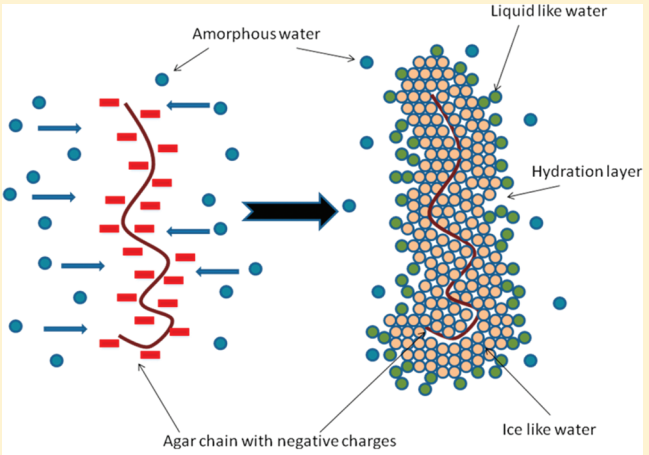

Hydration of agar chain in glycerol-water binary solvent

1. INTRODUCTION

Organogels constitute a diverse group of gelled materials in which the immobilized liquid is nonaqueous.[1] These systems have experienced an enormous increase in interest during the past decade.[2−11] The organogels of chemical origin consist of low concentration of one or more low-molecular-mass organogelators that self-assemble to form a semirigid three-dimensional network in an organic solvent.[2] These systems constitute an important class of materials due to their applications in templated material synthesis,[3,4] entrapment of biomolecules,[5] separations,[6] photoinduced charge transfer,[7,8] and biomimetics.[9] However, recently a lot of attention was given to the biopolymeric organogels due to their biocompatibility and negligible level of cytotoxicity.[10,11] These gels have found use in relevant drug delivery applications. Microemulsion-based organogels belong to a special category of soft matter, and their special features are extensively reviewed by Atkins et al.[12]

Agar comprises mainly of alternating β-(1−4)-D and α-(1−4)-L linked galactose residues in a way that most of the α-(1−4) residues are modified by the presence of a 3,6 anhydro bridge. Other modifications commonly observed are mainly substitutes of sulfate, pyruvate, urinate or methoxyl groups. The gelation temperature of agar is primarily decided by the methoxy content of the sample. Agar sols form thermo-reversible physical gels with large hysteresis between melting ($T_m \approx 85$ °C) and gelling ($T_g \approx 40$ °C) temperatures with the constituent unit being antisymmetric double helices. Glycerol, a trihydric alcohol, is used by a number of organisms for its cryoprotective properties.[13,14] In nature, glycerol is used in high concentrations as a colligative cryoprotectant that raises the osmolality of body fluids and reduces the water available to form extracellular ice.[15] Glycerol is also active in maintaining the structure of biological macromolecules and in promoting protein self-assembly through preferential hydration.[16] Experimentally, the glass-forming properties of high glycerol−water mixtures have made these solutions an attractive solvent system for low temperature studies of proteins. The glycerol−water

Received: March 7, 2012
Revised: May 30, 2012
Published: June 1, 2012

dx.doi.org/10.1021/jp3022024 | J. Phys. Chem. B 2012, 116, 7113−7121

system is the fluid of choice if one wants to easily vary the viscosity of a fluid over a large range due to its hydrogen bonding (H-bonding) nature. Hydrogen bonding liquids and their mixtures occupy a special place among complex systems due to the existence of directed H-bonds. In contrast to covalent bonds, the H-bonds can be rearranged relatively easily. Although an enormous amount of literature exists which relates to the investigation of H-bonding systems, particularly on glycerol−water mixture systems,[17−23] there is still a lack of clear understanding even on the level of dynamics in "simple" water or alcohols. Among them, glycerol and its mixtures with water are widely used as excellent models to study cooperative dynamics.

Agar, a polyanionic carbohydrate, is extensively studied due to its gelling ability at low concentrations.[24−27] Considerable effort has been made to understand the intricacies of its gelation dynamics and mechanism.[24,25] Agar organogels in glycerol solutions is a new kind of soft matter system and in a bid to probe this system in details the present work was carried out. In an earlier work, we reported gelatin organogels in glycerol solutions that had unique attributes.[26] A comparison between the two organogels reveals very interesting features.

II. MATERIALS AND METHODS

Powdered agar was generously provided by Centre for Salt and Marine Minerals Research Institute, Bhavnagar, India. A further detail about this sample is provided in ref 24. Triple deionized water from Organo Biotech Laboratories, India, was used to prepare the solutions. Seven solvents of water $(100 - x)$−glycerol (x) binary mixture were prepared with concentration of glycerol x (% v/v) varying from 0 to 60. The solutions were prepared by autoclaving the agar powder in required glycerol−water mixture at 120 °C and high pressure with concentrations varying from 0.02% to 0.3% (w/v), and these were homogenized by 10 min of stirring while hot. These samples were allowed to cool spontaneously through Newtonian cooling and to form gels. The gel samples appeared optically clear and transparent to the eye and did not contain air bubbles. These were stored in a borosilicate glass bottles at room temperature (20 °C). All experiments on gels were performed on one week old samples which was felt necessary to ensure sample homogeneity.

Raman spectra of glycerol−water binary solvent, agar in glycerol solutions, and agar organogels wereaaawq recorded on a FT-IR/Raman spectrometer with microscopes: Varian 7000 FTIR, Varian FT-Raman, and Varian 600 UMA. We have adopted Raman spectroscopy to investigate structure of water in all the systems because vibrational spectra are very sensitive to the local molecular environment. DLS experiments were performed at scattering angle of $\theta = 90°$ and laser wavelength of λ = 632.8 nm on a 256-channel Photocor-FC (Photocor Inc., U.S.A.) that was operated in the multi-τ mode (logarithmically spaced channels). The goniometer was placed on a Newport (U.S.A.) vibration isolation table. The agar concentration used was 0.02% (w/v) for all glycerol concentrations in the measurement of apparent hydrodynamic radius of the biopolymer molecule (R_h). The time scale spanned 8 decades, i.e., from 0.5 μs to 10 s. The samples were housed inside a thermostatic bath, and the temperature was regulated by a PID temperature controller to an accuracy of ±0.1 °C. In all experiments, the difference between the measured and calculated baseline was not allowed to go beyond ±0.1%. The data that showed excessive baseline difference were rejected. Analysis of the measured correlation function yields the translational diffusion coefficient of the scattering moiety. The diffusion coefficient is related to corresponding effective hydrodynamic radius through the Stoke−Einstein relation

$$D = \frac{k_B T}{6\pi\eta_0 R_h} \quad (1)$$

where the solvent viscosity is η_0, k_B is the Boltzmann constant, and T is the absolute temperature.

Viscosity values were measured using a vibro viscometer (model-SV10, A & D Co., Japan). This instrument uses a matched pair of gold plated flat electrodes. The mechanical vibrations (frequency ≈ 30 Hz) set in one of these propagate through the sample and is picked up by the other electrode. The viscoelastic properties of the sample are deduced from the response function through the software provided by the manufacturer. Rheology experiments were performed using an AR-500 model stress controlled rheometer (T.A. Instruments, U.K.) with the objective to inter-relate the stiffness and thermal stability of the networks in frequency and temperature sweep modes. The temperature sweep modes (heating rate 5 °C/min) were measured using the cone geometry (20 mm diameter, 2° cone angle, and 56-mm truncation gap) at fixed angular frequency of 6.2830 Hz and controlled stress of 4.7750 Pa. The details of the experiment are similar as described in our earlier work with agar hydrogels.[24] The frequency sweep experiments were performed on the gel samples using parallel-plate geometry (20 mm diameter, 2° cone angle, and 58-mm truncation gap) with constant oscillatory stress value as 6.3 Pa at different temperatures ranging from 20 to 40 °C. Circular dichroism experiments were carried out on 0.02% (w/v) agar in all glycerol−water solvents with an Applied Photophysics Chirascan instrument (USA) to estimate the degree of helicity.

III. RESULTS AND DISCUSSION

1. Structure of Water from Raman Studies. The Raman peaks were seen to occur in two distinct frequency bands: 600−2000 and 3050−3800 cm^{-1}. The main focus of these studies was to explore the hydration of agar in glycerol solutions. Thus, the Raman bands residing in the frequency band 3050−3800 cm^{-1} were of interest as these pertain to various O−H stretching modes. A detailed discussion on the deconvolution of raw Raman spectra is provided in ref 26. We have followed identical procedure while treating Raman data obtained from various samples studied in this work.

a. Water Structure in Glycerol Solutions. Evaluation of the hydration of glycerol molecules in glycerol solutions is very essential before we proceed to understand the solvation of agar in glycerol solution. Glycerol−water system has been subjected to enormous number of studies in the past using Raman spectroscopy.[28−35] The Raman spectra, occurring in the frequency band 2800−3800 cm^{-1}, obtained from glycerol solutions were fitted to three-peak Lorentzian functions that resolved the O−H stretching peaks located at 3200, 3310, and 3460 cm^{-1}. These peaks represent the ice-like water structure (fully structured), liquid-like water structure (partially structured) and amorphous water structure (free water) respectively. The spectral analysis was robust that made us believe that the peaks in question were resolvable through sufficient statistical accuracy (χ^2 >0.97). Representative deconvolution of Raman spectra are shown in the Supporting Information (Figure S1).

dx.doi.org/10.1021/jp3022024 | J. Phys. Chem. B 2012, 116, 7113−7121

From the deconvolution of the Raman spectra the area fractions of the three aforesaid bands were determined, which is shown in Figure 1. We see that the ice-like structure is

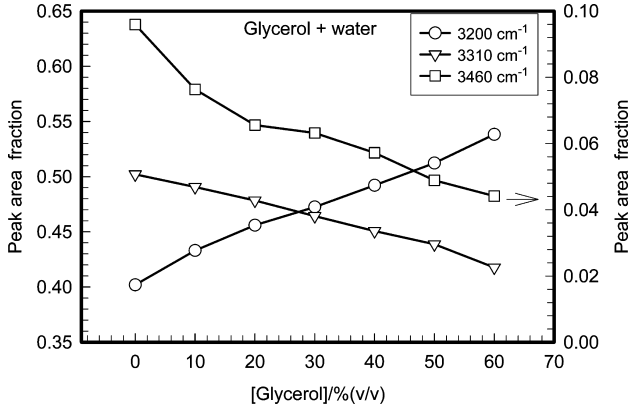

Figure 1. Fractional area of various Raman bands for the glycerol–water solvent showing an increase in the ice-like structure of water increasing with glycerol concentration while the fractions of partially structured and amorphous water decreasing with the same.

increased (by ~40%) while the partially structured fraction is decreased (by ~20%) with increase in glycerol concentration. These fractions owe their origin to the specifics of the hydrogen bonding between glycerol and water molecules. This data needs to be explained in details.

We propose a hydration model and hypothesize that the specific hydration of oxygen atoms by available hydrogen atoms in the system dictates the area of various Raman bands. Specifically, when the O-atom has all four bonds (including the covalent and H-bonds) engaged with four H-atoms, we describe it as fully structured, when three bonds are engaged with three different H-atoms, it is partially structured and when only two bonds are engaged with two H-atoms, we refer to it as free water molecule. The ratio of H-atoms available for hydrogen bonding to O-atoms in the system was calculated for various concentrations of glycerol and the same is shown in Figure 2. Here, we see that the hydration of O_w (O-atoms of

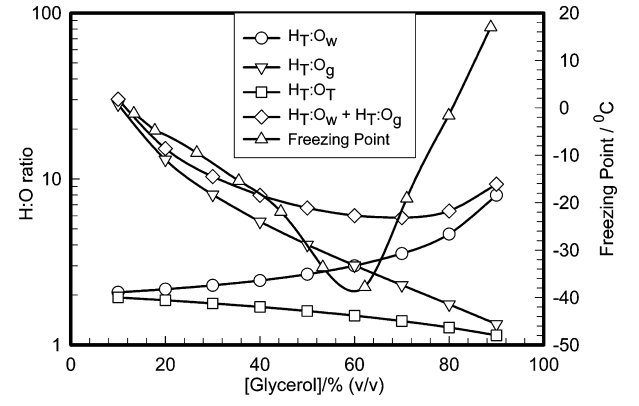

Figure 2. Plot of hydrogen atom to oxygen atom (H:O) ratio shown as function of glycerol concentration. H_T and O_T represent the total number of H-atoms and O-atoms available for H-bonding respectively, and O_w and O_g represent the total number of O-atoms in water and glycerol, respectively. Note the freezing point is a minimum at 60% v/v glycerol concentration where H_T:O_w + H_T:O_g is a minimum. See the text for details.

water) increases, whereas hydration of O_g (O-atoms of glycerol) decreases with increase in concentration of glycerol in the solution. The hydration to the O-atoms is provided by the total number of H-atoms (H_T) present. Thus, the ratios H_T:O_w and H_T:O_g are relevant parameters that quantify hydration. So one can clearly conclude that O_w contributes more to the ice-like structure and O_g contributes predominantly to the partially structured water by comparing the data presented in Figures 1 and 2. Figure 2 data reveals that the H_T:O_w ratio increases and the H_T:O_g ratio decreases in the system with a rise in glycerol concentration. Thus, one can visualize why the concentration of ice-like structure in the system increases with increase in glycerol concentration (Figure 1). Near 60% (v/v) glycerol concentration, one observes that the ratios H_T:O_w and H_T:O_g are equal and their sum is minimum predicting that here the system has minimum hydration. At this point, one finds the freezing point minimum in the glycerol–water mixture[36] (Figure 2). Thus, in summary, we may conclude that hydration of O_w atoms is responsible for contributing to fully structured water and hydration of O_g atoms is responsible for partially structured water. The peak area fractions for the amorphous water structure were found in traces within 10% of the entire options available to an O-atom, which may be accommodated as a statistical error in our aforesaid hypothesis. The hypothesis agrees with the reports in the literature that confirm that the presence of glycerol enhances the water structure.[28−30] See the Supporting Information for obtaining further insight into the model (Figure S2).

b. Water Structure in Agar Organo Solutions. Now we come to the system of agar organo solutions where we have chosen two categories, of which one system is in solution phase (0.02% w/v) and the other comprises the gel phase (0.3% w/v). Before making any remarks on the hydration analysis, we should remember the structure of agar where a number of O-atoms are available for hydrogen bonding with solvent molecules. These O-atoms participate in the O–H stretching modes probed by Raman spectroscopy. Agar is soluble in glycerol unlike the case for gelatin.[26] Thus, there is the possibility of hydration of agar molecules by the glycerol molecules mostly through hydrogen bonding unlike in the case of the gelatin–glycerol–water system.[26] The peak area fractions analyzed through Raman spectra for the solution phase is depicted in Figure 3 where we find that the fraction of fully structured water is decreasing while the partially structured structure is increasing with glycerol concentration.

The Raman data shown in Figure 3 indicates that there was substantial gain in the partially structured water (by ~50%) which was compensated by a loss in structured water (~35%). This imbalance (as compared to the data shown in Figure 1) was due to the selective hydration of agar molecule in the mixed solvent environment. The aforesaid feature can be explained as follows. The structure of one unit (monomer) of agar has nine O-atoms of which five O-atoms (attached to ether groups) contribute to the formation of amorphous structures by forming H-bond with water or glycerol molecules, whereas four O-atoms attached to −OH groups will contribute to the formation of partially structured water. Since the agar content is small (0.02% w/v), the contribution of hydration of these O-atoms in agar in the observed Raman spectra should be marginal if the hydrogen to oxygen (H:O) ratio is considered as discussed earlier for the glycerol–water case. Yet considerable structural changes in hydration are observed which are different

dx.doi.org/10.1021/jp3022024 | J. Phys. Chem. B 2012, 116, 7113–7121

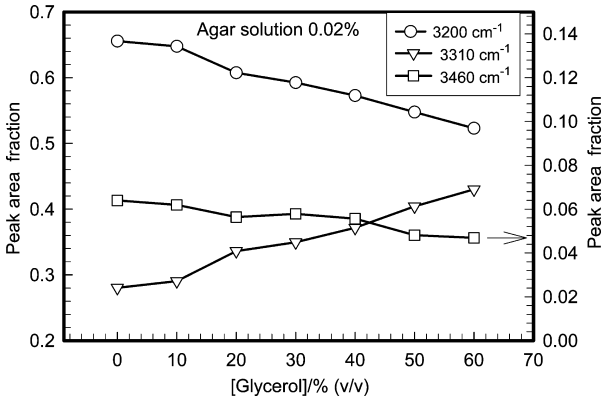

Figure 3. Raman spectra for 0.02% (w/v) agar in glycerol solution showing a decrease in the ice-like structure with increasing concentration of glycerol, a feature that was opposite to what was seen in Figure 1.

from the systems in absence of agar. Agar is highly electronegative whose zeta-potential was measured to be around −20 mV.[27] This electronegativity in agar is responsible for its chain stiffness and the presence of a large sheath of hydration layer around it. The water molecules participating in this hydration sheath are mostly the ice-like structure of water, and H-bonded glycerol and water molecules contribute to the second hydration layer formed by partially structured water. Some water not participating in the hydration layer around agar also contributes to the ice-like structure of the bulk solvent but these are less in number. A schematic diagram representing the proposed chain hydration is shown in Figure 4.

Dynamic light scattering experiments performed on 0.02% agar in glycerol solutions reveal that the hydrodynamic radius of the agar increases with an increase in glycerol concentration from 200 to 600 nm at 40% (v/v) glycerol concentration (plot provided in the Supporting Information, Figure S3). As the glycerol concentration is increased, the hydration sheath around agar decreases with no change in electronegativity of agar due to redistribution of solvent molecules. More specifically, there is a competition between the glycerol and agar molecules to pull water molecules toward each other. Being a small molecule in front of a giant agar molecule, glycerol molecules remain near the water molecules already attached with the agar molecule in the hydration sheath and move with the agar chain as part of the same moiety. In other words, the increase in glycerol content nullifies the effect of the presence of agar molecules in the system as the peak area fraction for ice-like structure drops to almost the same point where the same was observed to rise as in the case of the glycerol−water system at 60% v/v glycerol concentration (Figure 2). This qualitatively explains the decrease in the ice-like structure and increase in partially structured structure of water with the increase in glycerol concentration in the agar solutions.

c. Water Structure in Organogel. Now considering the organogel phase, we see a completely different scenario. The environment in solution phase is structurally different to that of the gel phase. It has been already reported earlier, that agar forms double helices and then bundles of such helices yield rod like structures that physically entangle to form statistical gels with no characteristic correlation length.[25] In gel phase the solvent is interstitially trapped inside the gel network causing the viscosity to go high and attributing viscoelasticity to the material. Since the H-bond is highly directional in nature, the ice-like structure has low mass density compared to liquid-like structure, thus there is a paucity of space for such large tetrahedral water structures to be accommodated inside network cages and consequently the trapped water is largely partially structured. This results in a drop in the peak area fraction of partially structured water in the Raman spectra as depicted in Figure 5. On addition of glycerol, the number of

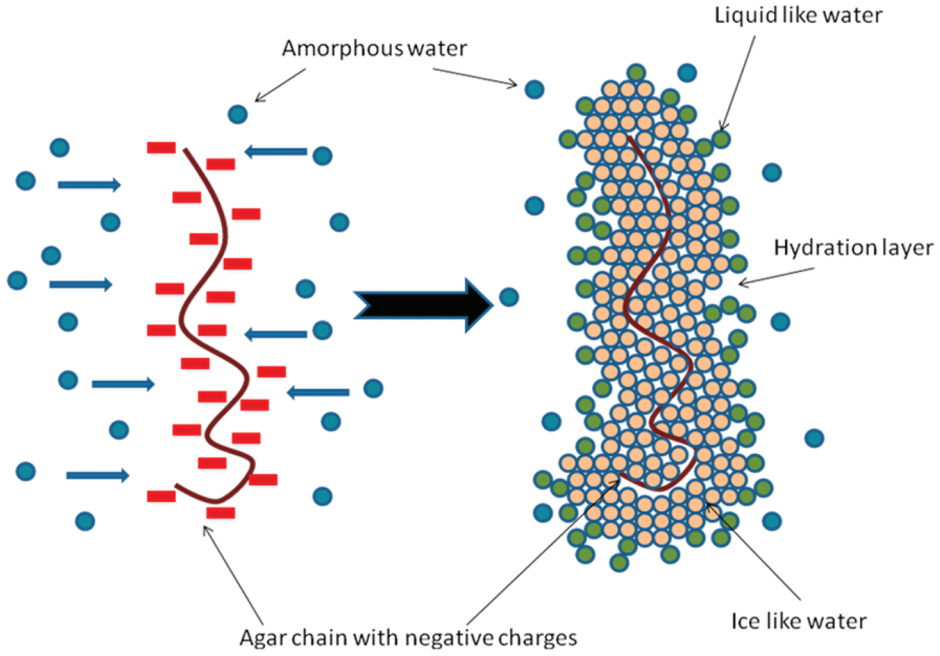

Figure 4. Schematic representation for hydration of thte agar chain in the glycerol−water solvent system. The left sketch depicts the nascent situation when agar is added to the solvent, and the right sketch shows equilibrium hydration. Notice the structured water hydration sheath around the agar chain.

dx.doi.org/10.1021/jp3022024 | J. Phys. Chem. B 2012, 116, 7113−7121

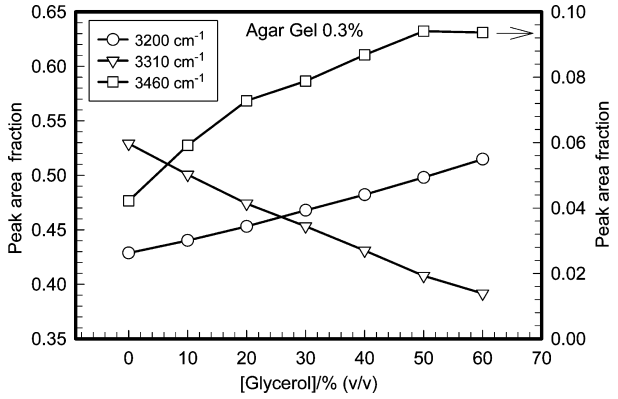

Figure 5. Raman spectra for 0.3% (w/v) agar organogels in glycerol solution indicating the depletion in the ice-like structure of water in the presence of the agar network (compare with Figure 3). However, this increases with addition of glycerol for a fixed agar content.

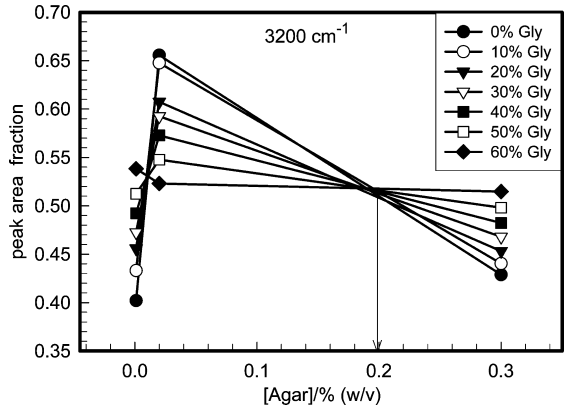

Figure 7. Peak area fraction for the Raman band for the frequency 3200 cm^{-1} (ice-like structure) with variation of agar concentration. Note the nullification of the effect of presence of glycerol near (0.2% w/v) which is the gelling concentration of agar (arrow).

water molecules decrease in the system and the system reorganizes the water and glycerol molecules within the gel network in such a way that the ice-like structure gets evolved with increase in glycerol concentration. Basically, the O_w is hydrated by H_T here as was the case in the water−glycerol system. A schematic diagram representing the hydration of the agar organogel system is shown in Figure 6.

At this stage it is imperative to ask what is the effect of agar concentration on water structure? We discuss this in the following using the experimental data depicted in Figure 7. It is very interesting to observe the variation of peak area fraction with agar concentration at different concentrations of glycerol for the ice-like structure. The effect of the presence of glycerol is invariant of the chain hydration in the system near 0.2% of agar (Figure 7) which is the gelling concentration for agar. The extent of the hydration layer around the polymer in the system plays a vital role in the formation of a gel. As the polymer concentration is increased, the hydration layer goes on decreasing until a point where it loses its identity. This point defines the gelation condition for the biopolymer. On further increase of polymer concentration, the entanglement of the polymer starts resulting in the formation of organogel. The entanglement points become static and the system evolves from an ergodic to a nonergodic phase. Thus, in case of a gel, the meaning of the hydration layer around the polymer chain, per se, loses its sense.

It is pertinent to compare the data shown in Figures 5 and 7 with similar observation made by Ratajska-Gadomska and Gadomski,[32] who deconvoluted their Raman spectra by fitting their data to 6-peak Guassian functions. The same spectral region was fitted to three Lorentzian functions in our case. This will clearly attribute more statistical weight to each of these three peaks compared to Ratajska-Gadomska and W. Gadomski result. This is clearly seen in Figures 5 and 7, with data pertaining to the ice-like structured water (3200 cm^{-1} band). Second, they observed an ~6% increase in the fractional area of

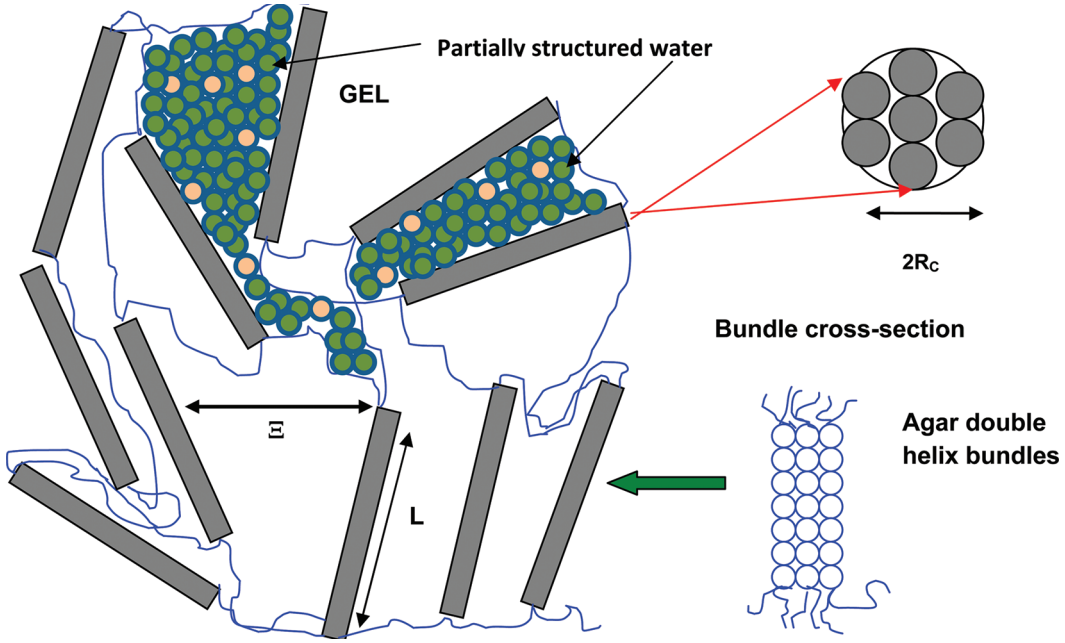

Figure 6. Schematic representation of the hydration of the physical network inside the organogel. Double helix length is L, and Ξ represents the interhelix distance. The cross-sectional radius is R_c. See ref 25 for details on the structure.

dx.doi.org/10.1021/jp3022024 | J. Phys. Chem. B 2012, 116, 7113−7121

this band (Table 1 of their paper) as the polymer concentration was raised from 1 to 4%. All of their samples were gelling sols, whereas in our case, we have only a single sample in that state (0.3%) and hence only one data point (Figure 7). Since hydration of biopolymers is strongly concentration dependent,[37] we are unable to provide a clear comparison.

2. Phase Diagram of Organogel. The viscosity of agar solutions was measured at 35 °C with concentrations varying from 0.02% to 0.3% in intervals of 0.02% (w/v). The gelling concentration C_g of agar for the various glycerol concentrations were determined by plotting the viscosity of agar solutions for various glycerol concentrations as shown in Figure 8. The

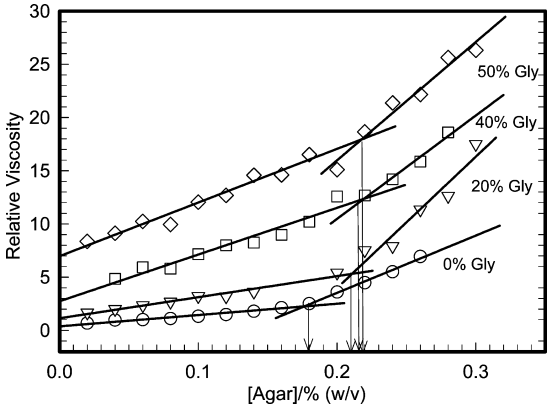

Figure 8. Determination of gelation concentration (C_g) for agar in various glycerol concentrations (arrows) determined from viscosity data recorded at 35 °C.

gelation concentration, C_g, was found to increase with glycerol concentration indicating that it is harder to form glycerol organogels. The gel strength is determined by the strength of the storage modulus (G'), and in a gel its value exceeds that of loss modulus (G'') by manifold. Both G' and G'' are dispersive in nature; their values depend on measurement frequency, ω.

The isochronal temperature sweep results performed on hot samples of 0.3% (w/v) agar sols revealed a hysteresis loop similar to that reported in our previous work.[24] In such a study, the $G'(\omega)$ is measured at a very low frequency and the corresponding modulus G_0' is evaluated as the gel strength parameter. The organogel exhibited a cyclic gelling-melting thermogram that clearly identified the two characteristic temperatures, T_g and T_m (inset Figure 9). The plot of dG_0'/dt versus T for heating phase of the cycle clearly establishes T_m temperature in Figure 10. Both the gelation and melting temperatures (T_g and T_m) were found to decrease with the increase in glycerol concentration (Table 1). We thus propose a 3D-phase plot for the organogels which is shown in Figure 11 using T_g data. Two distinctive features are evident here: (i) presence of glycerol as a cosolvent does not favor the gelation of agar as compared to water and (ii) agar organogels are softer than their hydrogels.

3. Viscoelastic Properties of Organogels. Organogels are soft matter with profound viscoelastic attributes which are best probed by dynamic rheology using temperature sweep and frequency sweep protocols. The temperature sweep studies revealed the thermal properties like gelling and melting temperatures of the organogels which has been already discussed. The mechanical properties were probed by subjecting these to frequency sweep studies.

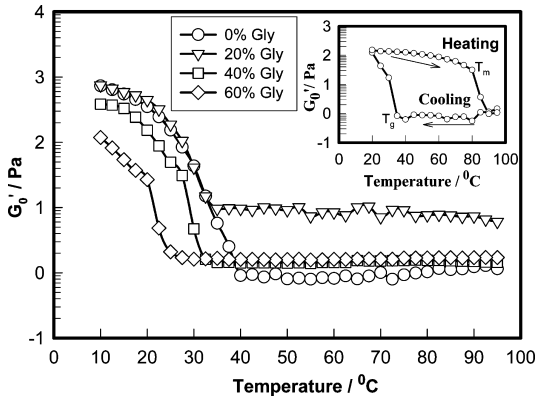

Figure 9. Variation of isochronal storage modulus, G_0', versus temperature for agar organogel samples; the inset shows the hysteresis path followed by a typical agar hydrogel.

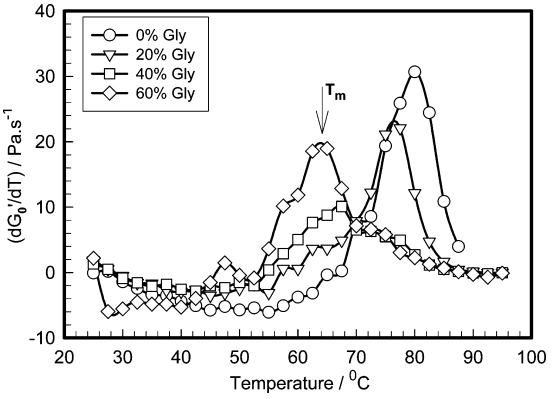

Figure 10. Plot for dG_0'/dT versus temperature for determination of melting temperature, T_m, for various samples. Arrow indicate typical transition temperature for a sample.

Table 1. Variation of Gelation Concentration, Gelation, and Melting Temperature of Organogels

glycerol concentration (% v/v)	C_g (% w/v)	T_g (°C)	T_m (°C)
0	0.180	40.0	81.0
10	0.185	35.0	80.0
20	0.210	34.0	76.5
30	0.215	34.0	68.5
40	0.220	33.0	67.5
50	0.220	28.0	65.0

Frequency sweep experiments were also performed on the 0.3% agar organogels at various temperatures ranging from 20 to 40 °C which is shown in Figure 12. The storage modulus, $G'(\omega)$, followed a power-law function

$$G'(\omega) \approx G_0'\omega^n \quad (3)$$

where the exponent n defines degree of network connectivity and G_0' characterizes gel strengths, and these are shown in Figures 13 and 14 (inset) for various samples. Interestingly, one can see that the G_0' of the system decreases with an increase in glycerol concentration, which supports the fact that glycerol weakens the network structure of the gel. The linear viscoelasticity model proposed by Winter[38] predicts that the stress-relaxation follows the power-law frequency dependence behavior given by eq 3 with $0 < n < 1$. Stoichiometrically balanced and imbalanced cross-linked networks showed $n < 1/$

dx.doi.org/10.1021/jp3022024 | J. Phys. Chem. B 2012, 116, 7113−7121

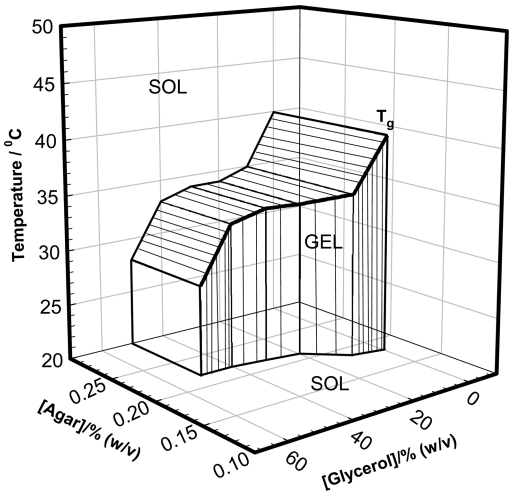

Figure 11. 3D phase diagram of agar organogels in glycerol solution with T_g. Note that the gelation concentration increases and gelation temperature reduces as glycerol concentration is increased in the solvent.

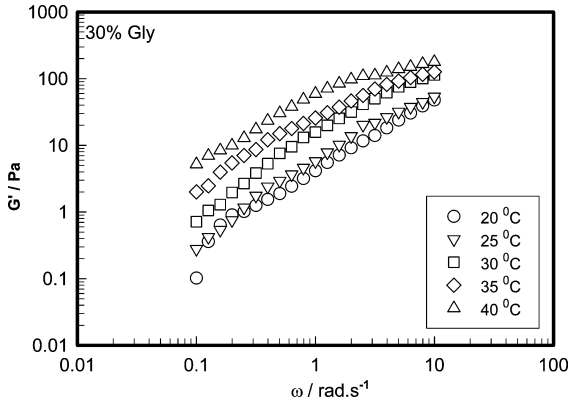

Figure 12. Representative frequency sweep plots for 0.3% (w/v) agar organogel system showing variation of storage modulus at various temperatures. Note the tendency of alignment of the curves predicting independence of the exponent, n, on temperature implying that the gels become softer with the addition of glycerol.

2 (excess cross-linker) and $n > 1/2$ (lack of cross-linker) respectively. This description strictly applies to chemically cross-linked gels, and thus the observation of $0.2 < n < 1$ for the

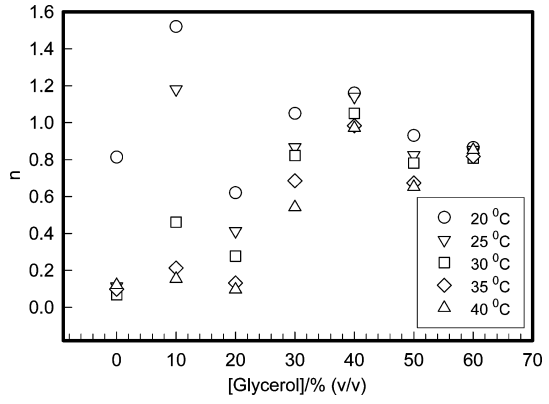

Figure 13. Variation of the exponent, n of the power-law function $G' \approx \omega^n$, with glycerol concentration shown for various temperatures.

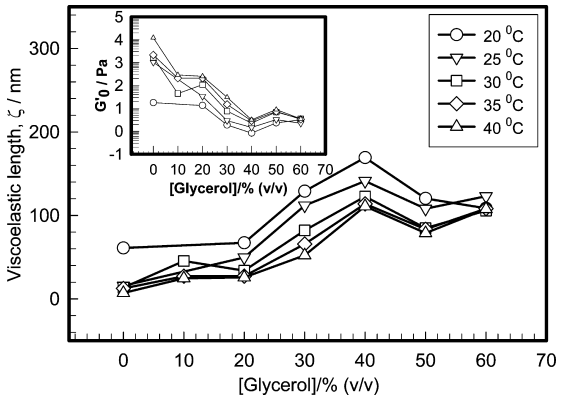

Figure 14. Viscoelastic length of the system increases with glycerol concentration, the inset showing the gel strength, and G_0 decreases with increase in glycerol concentration supporting the softening of the gel with addition of glycerol.

present systems where no cross-linker is present per se does not come as a surprise. A theoretical rheological model for agar gels was proposed by Labropoulos et al.[39] that assumes temperature dependence of monomer friction coefficient of agar molecules which allows net association rate enroute to gelation to be estimated from time−temperature data. Rheological measurements, using a dynamic mechanical analyzer, carried out by Chen et al[40] in the frequency sweep shear sandwich mode (0.1−20 Hz) revealed that $|G^*| \approx \omega^n$ with n ranging between ∼0.025 and 0.035 which allowed the agar gels to be modeled within the fractional derivative framework. These results indicate that power-law exponent can assume a range of values.

The viscoelastic lengths ζ for various systems were determined from the relation[41]

$$G_0 = k_B T/\zeta^3 \quad (4)$$

where G_0 is the value of G' at the angular frequency of 0.5012 rad/s (Figure 13).

It was observed that as the glycerol concentration increased in the solvent, the power-law exponent, n, increased gradually and finally at 60% w/v glycerol, there was complete independence with temperature, which means the organogels became more and more viscous (liquid-like) with increase of glycerol concentration, supporting again the conclusion that glycerol weakens the gel network.

4. Biological Activity of Agar. It is pertinent to establish that glycerol solutions do not affect the biological integrity of agar molecules. This is best resolved through observing its secondary structure. The circular dichroism experiments performed on these same samples (Figure 15) revealed that the helicity of this biopolymer remained unchanged in the glycerol environment.

6. Comparison between Agar and Gelatin Organogels. Glycerol interacts differently with agar and gelatin biopolymers. For agar, it is a solvent, whereas for gelatin it acts as a nonsolvent. Hence the organogels obtained from both these polymers with the same solvent of glycerol−water binary mixture show different thermophysical attributes. Table 3 gives an overview of comparison between the two organogels. The hydrodynamic radius R_h and gelling concentration C_g increase with glycerol concentration in agar organogels while in case of gelatin organogel, they decrease. The T_g and T_m and gel strength (G_0') decreases in former system,, whereas they increase in later. The ice-like water structure in the solution

dx.doi.org/10.1021/jp3022024 | J. Phys. Chem. B 2012, 116, 7113−7121

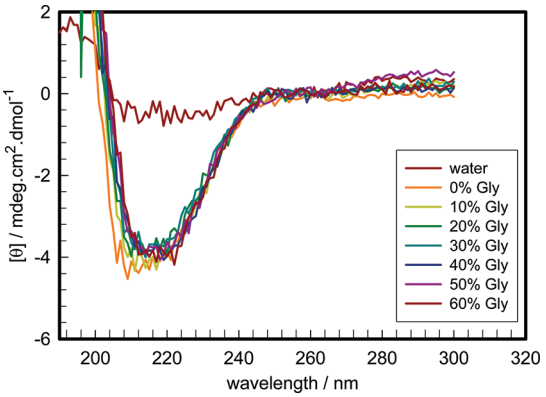

Figure 15. Circular dichorism spectra of agar (0.02% w/v) dissolved in glycerol solutions. Note the invariance of spectral profile with glycerol concentration implying that the biological activity of the molecules remains unaltered.

Table 3. Comparison of Agar and Gelatin Organogels with Increase in Glycerol Concentration

S. no.	properties	agar organogel	gelatin organogel[26]
1	apparent chain size	increases	decreases
2	solvent nature, glycerol	solvent	nonsolvent
3	zeta potential	no variance	decreases
4	ice-like structure, (3200 cm^{-1})	decreases (in solution phase)	increases (in solution phase)
		increases (in gel phase)	____
5	liquid-like structure, (3310 cm^{-1})	increases (in solution phase)	decreases (in solution phase)
		decreases (in gel phase)	____
6	gelation conc.	increases	decreases
8	gelation temperature	decreases	increases
9	gel strength,	decreases	increases
10	network structure	gets softer	gets stronger

phase in the gelatin system decreases, whereas in the agar system, it increases with the increase of glycerol content. The gel strength decreases in the former and increases in later system, confirming the network structure getting softer in former and stronger in later system.

IV. CONCLUSION

Raman data helps us to explore the water structure involved in solvent, solution, and gel phases. In our proposed hydration model, the ice-like water structure is contributed by the oxygen present in the water molecule, whereas the liquid like structures are contributed by oxygen atoms of both glycerol and water molecules. In the binary solvent system the probability of formation of ice-like structure by O-atom in water molecule increases due to availability of more hydration to it, but such O-atoms decreases in number with increase in glycerol concentration. In solution phase, since the number of agar molecules is very less, the contribution of O-atoms present in agar to alter the structure of the system is very less if the H:O ratio is considered. The polyanionic nature of agar plays here a major role by formation of hydration layer around it which contributes mainly to the ice-like structure. On increase of glycerol concentration, this ice-like structure in hydration layer is disturbed by glycerol molecules; hence a decrease in propensity of the same is seen. In organogel phase, the concept of hydration layer is lost and the solvent molecules are trapped in small cages tightly which is not conducive to the ice-like structure formation due to paucity of physical space. On increase of glycerol content the hydration is provided more to the O-atoms of water molecules which increases the fraction of ice-like water structure in organogel system. At a threshold concentration of agar (~0.2% w/v), the effect of hydration showing dependence on glycerol concentration was not observed in Raman data. This was identified as gelation concentration where the concept of hydration layer of individual chains is almost lost and the network structure of polymer comes into existence with its characteristic different hydration features. Here some glycerol molecules provide hydration to O-atoms of water to form ice-like structures and some pull out water molecule from agar hydration layer to give a liquid-like structure in such a way that the fraction of ice-like structure is the unaltered.

The viscosity studies indeed predicted the cluster formation/aggregation of agar molecules in the system but these do not confirm the formation of any network structure in the system. Rather from the experimental data, gelation concentration was found to increase with glycerol content. Had the C_g value decreased with increase of glycerol concentration, one would have generated stronger organogels at same agar concentration. But on the contrary, one can see from the frequency sweep data that the gel strength decreased with increase of glycerol concentration resulting in weaker and weaker gels. However, the DLS studies predicted the cluster formation/aggregation of agar molecules with increase of glycerol concentration. Agar and gelatin molecules were observed to hydrate differently in glycerol solutions which gave rise to organogels having contrastingly different thermo-mechanical properties. More experiments need to be done with other biopolymeric sols and gels in organic solvents to generate a universal understanding of hydration of organogels vis a vis water structure.

■ ASSOCIATED CONTENT

Ⓢ Supporting Information

Further details of deconvolution of Raman spectra, H-bonding model, and variation in apparent size of agar molecule in glycerol solutions are provided. This material is available free of charge via the Internet at http://pubs.acs.org.

■ AUTHOR INFORMATION

Corresponding Author

*E-mail: bohi0700@mail.jnu.ac.in. Fax: +91 11 2674 1837. Tel: +91 11 2674 4637.

Notes

The authors declare no competing financial interest.

■ ACKNOWLEDGMENTS

We are thankful to Advanced Research Instrumentation Facility of the University for allowing us access to the Raman and CD facility. S.B. acknowledges the Council of Scientific and Industrial Research, India for a Senior Research Fellowship.

■ REFERENCES

(1) Wright, A. J; Marangoni, A. G. *J. Am. Oil Chem. Soc.* **2006**, *83*, 497−503.
(2) Abdallah, D, J.; Weiss, R,G. *Adv. Matter* **2000**, *12*, 1237−1247.
(3) Rees, G,D.; Robinson, B. H. *Adv. Matter* **1993**, *5*, 608−619.
(4) Loos, M.; Esch, J.; Stokroos, I.; Kellogg, R. M.; Feringa, B. L. *J. Am. Chem. Soc.* **1997**, *119*, 12675−12676.

(5) Haering, G.; Luisi, P. L. *J. Phys. Chem.* **1986**, *90*, 5892−5895.
(6) Phillips, R. J.; Deen, W. M.; Brady, J. F. *J. Colloid Interface Sci.* **1990**, *139*, 363−373.
(7) Ajayaghosh, A.; George, S. J.; Praveen, V. K. *Angew. Chem.* **2003**, *42*, 332−335.
(8) Shirakawa, M.; Fujita, N.; Shinkai, S. *J. Am. Chem. Soc.* **2003**, *125*, 9902−9903.
(9) Hafkamp, R. J. H.; Kokke, B. P. A.; Danke, I. M.; Guerts, H. P. M.; Rowan, A. E.; Feiters, M. C.; Nolte, R. J. M. *Chem. Commun.* **1997**, 545−546.
(10) Nostro, P. L.; Ambrosi, M.; Ninham, B. W.; Baglioni, P. *J. Phys. Chem. B* **2009**, *113*, 8324−8331.
(11) Kumar, R.; Katare, O. P. *AAPS PharmSciTech* **2005**, *6*, E298−E310.
(12) Atkins, P. J.; Clark, D C.; Howe, A. M.; Heenan, R. K.; Robinson, B. H. *Prog. Colloid Polym. Sci.* **1991**, *84*, 129−132.
(13) Izawa, S.; Sato, M.; Yokoigawa, K.; Inoue, Y. *Appl. Microbiol. Biotechnol.* **2004**, *66*, 108−114.
(14) Izumi, Y.; Sonoda, S.; Yoshida, H.; Danks, H. V.; Tsumuki, H. *J. Insect Physiol.* **2006**, *52*, 215−220.
(15) Storey, K. B. *Comp. Biochem. Physiol.* **1997**, *117A*, 319−326.
(16) Davis-Searles, P. R.; Saunders, A. J.; Erie, D. A.; Winzor, D. J.; Pielak, G. J. *Annu. Rev. Biophys. Biomol. Struct.* **2001**, *30*, 271−306.
(17) Behrends, R.; Fuchs, K.; Kaatze, U.; Hayashi, Y.; Feldman, Y. *J. Chem. Phys.* **2006**, *124*, 144512−1−8.
(18) Shankar, P. N.; Kumar, M. *Proc. R. Soc. London A* **1994**, *444*, 573−581.
(19) Cheng, N. S. *Ind. Eng. Chem. Res.* **2008**, *47*, 3285−3288.
(20) Streit, S.; Sprung, M.; Gutt, C.; Tolan, M. *Physica B* **2005**, *357*, 110−114.
(21) Hayashi, Y.; Puzenko, A.; Balin, I.; Ryabov, Y. E.; Feldman, Y. *J. Phys. Chem. B* **2005**, *109*, 9174−9177.
(22) Dashnau, J. L.; Nucci, N. V.; Sharp, K. A.; Vanderkooi, J. M. *J. Phys. Chem. B* **2006**, *110*, 13670−13677.
(23) Towey, J. J; Soper, A. K.; Dougan, L. *J. Phys. Chem. B* **2011**, *115*, 7799−7807.
(24) Boral, S.; Saxena, A.; Bohidar, H. B. *J. Phys. Chem. B* **2008**, *112*, 3625−3632.
(25) Boral, S.; Bohidar, H. B. *Polymer* **2009**, *50*, 5585−5588.
(26) Sanwlani, S.; Kumar, P.; Bohidar, H. B. *J. Phys. Chem. B* **2011**, *115*, 7332−7340.
(27) Boral, S.; Bohidar, H. B. *J. Phys. Chem. B* **2010**, *114*, 12027−12035.
(28) Timasheff, S. N. *Adv. Protein Chem.* **1998**, *51*, 355−432.
(29) Singer, S. J. *Adv. Protein Chem.* **1963**, *17*, 1−68.
(30) Mudalige, A.; Pemberton, J. E. *Vibr. Spectrosc.* **2007**, *45*, 27−35.
(31) Carey, D. M.; Korenowski, G. M. *J. Chem. Phys.* **1998**, *108*, 2669−2775.
(32) Gadomski, W.; Ratajska-Gadomska, B. *Chem. Phys. Lett.* **2004**, *399*, 471−474.
(33) Ratajska-Gadomska, B.; Gadomski, W. *J. Chem. Phys.* **2010**, *133*, 234505−1−7.
(34) Gekko, K.; Timasheff, S. N. *Biochemistry* **1981**, *20*, 4667−4676.
(35) Adamenko, I. I.; Bulavin, L. A.; Ilyin, V.; Zelinsky, S. A.; Moroz, K. O. *J. Mol. Liq.* **2006**, *127*, 90−92.
(36) Our calculations show that freezing point minima exactly occur at a specific organic solvent concentration where the condition $(H_T{:}O_W + H_T{:}O_X) = 6 \pm 0.2$ is satisfied, where x represents the organic solvent, H_T is the total number of hydrogen atoms, and O_W and O_X represent number of oxygen atoms in water and organic liquid, respectively. Such a simple concept sufficiently and universally describes freezing point minima in ethylene glycol, methanol, ethanol, and iso-propanol solutions.
(37) Arfin, N.; Bohidar, H. B. *Int. J. Biol. Macromol.* **2012**, *50*, 759−767.
(38) Winter, H. H. *Polym. Eng. Sci.* **1987**, *27*, 1698−1702.
(39) Labropoulos, K. C.; Niesz., D E.; Danforth., S. C.; Kevrekidis, P. G. *Carbohydr. Polym.* **2002**, *50*, 393−406 and ibid 407−415..
(40) Chen, Q.; Suki, B.; An, K. N. *J. Biomech. Eng.* **2004**, *126*, 666−671.
(41) Ajji, A.; Choplin, L. *Macromolecules* **1991**, *24*, 5221−5223.